Electronic Supplementary Information

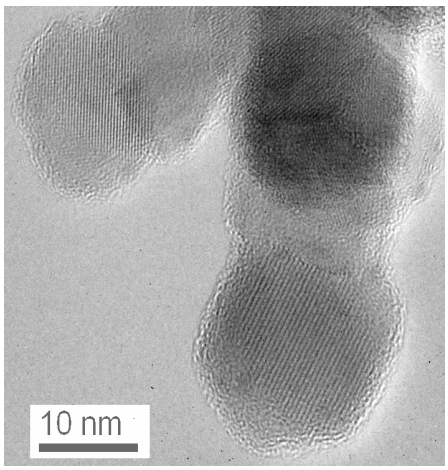

Fig. S1 TEM image of MIP-coated TiO_2 (4CP-P25) particles (obtained on a JEM-2010FEF TEM).

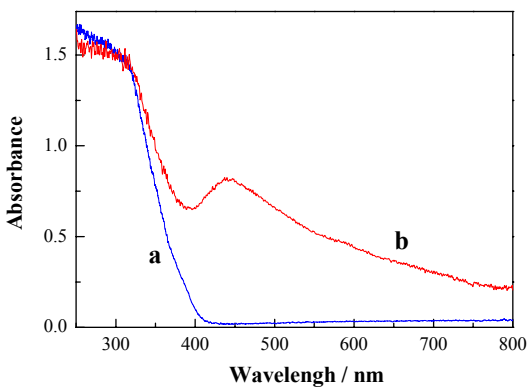

Fig. S2 UV-visible absorption spectra of P25 (a) and 4CP-P25 (b) particles. The spectra were detected on a Shimadzu UV-2550 spectrophotometer. It is easily seen that the MIP layer yielded absorption in the visible region with a maximum absorption at about 440 nm, which is attributed to the coated polymer of o-phenylenediamine.

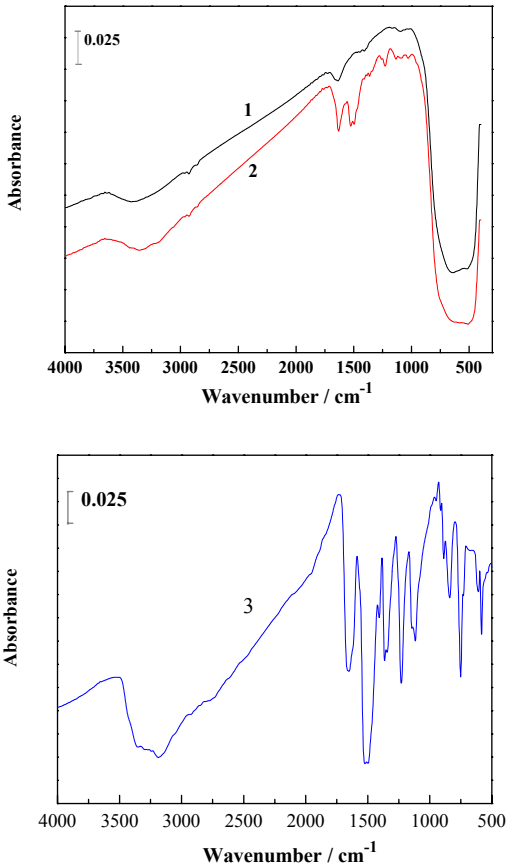

Fig. S3 FTIR spectra of P25 (1), 4CP-P25 (2) particles, and the polymer of OPDA (3) detected on a Bruker VERTEX 70 spectrophotometer. The MIP layer here was somewhat thicker than that required in practice, in order to clear show the absorption bands of the MIP layer.

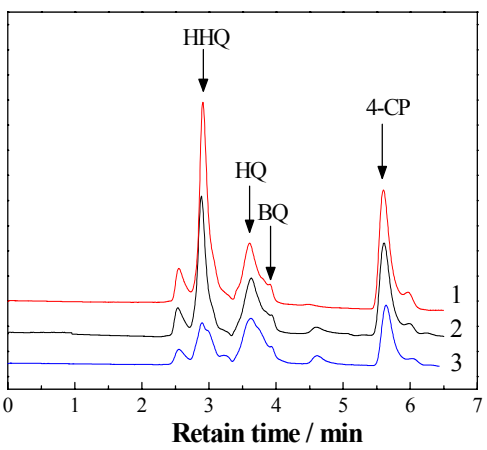

Fig. S4 HPLC diagrams of 4CP solutions (c_0 =184.3 μmol L^{-1}) after an UV light illuminating for 37.5 min in the absence of any photocatalyst (1), in the presence of P25 (2) and 4CP-P25 (3) as photocatalyst. The remained concentration of 4CP was determined as 77.6, 60.0, and 39.2 μmol L^{-1} for curves 1, 2 and 3, respectively. The main aromatic intermediates include HHQ (2-hydroxy-1,4-benzoquinone), HQ (1,4-hydroquinone) and BQ (1,4-benzoquinone).

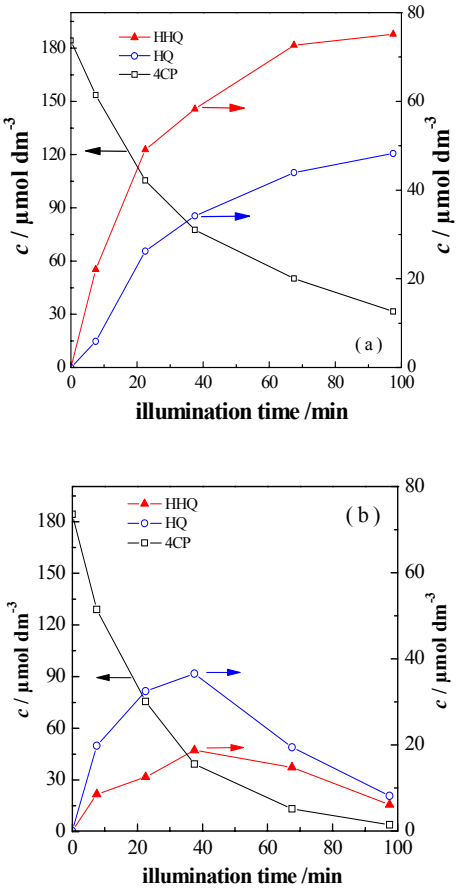

Fig. S5 Variations of main aromatic intermediates during the direct photolysisof 4CP (a) and the photocatalytic degradation of 4CP over 4CP-P25 (b).

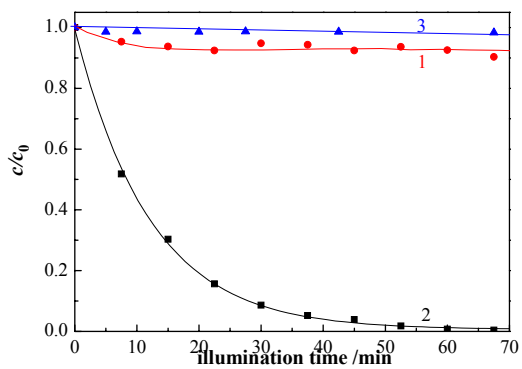

Fig. S6 Degradation kinetics for 4CP during the degradation in the mixtures of 4CP and phenol (c_0 = 2 mg L^{-1} for 4CP and 500 mg L^{-1} for phenol) under UV light illumination in the absence (1) and presence (2) of 4CP-P25 as photocatalyst. Curve 3 gave the variation of 4CP concentration in the presence of 4CP-P25 under dark, which indicated that the adsorption of 4CP on the surface of the photocatalyst 4CP-P25 did not influence the decrease of 4CP concentration.

310